INVITED PAPER

Thermal Interface Materials: Historical Perspective, Status, and Future Directions

Polymeric materials filled with heat-conducting particles can lower microelectronics operating temperatures by reducing the thermal resistance between chip surfaces and substrates.

By Ravi Prasher

ABSTRACT | With the continual increase in cooling demand for microprocessors, there has been an increased focus within the microelectronics industry on developing thermal solutions. Thermal interface materials (TIMs) play a key role in thermally connecting various components of the thermal solution. Review of the progress made in the area of TIMs in the past five years is presented. The focus is on the rheology-based modeling and design of polymeric TIMs due to their widespread use. Review of limited literature on the thermal performance of solders is also provided. Merits and demerits of using nanoparticles and nanotubes for TIM applications are also discussed. I conclude the paper with some directions for the future that I feel are relatively untouched and potentially very beneficial.

KEYWORDS | Bond line thickness (BLT); nanoparticles; nanotube; polymer rheology; thermal boundary resistance; thermal interface material (TIM)

NOMENCLATURE

R_{cs}	Contact resistance between two bare solids
R_{cTIM}	Contact resistance of an ideal TIM
H	Hardness
P	Pressure
m	Mean asperity slope
k_{TIM}	Thermal conductivity of the TIM
k_p	Thermal conductivity of particles (fillers)
k_m	Thermal conductivity of the polymer matrix
R_{TIM}	Thermal resistance of TIM (same as impedance)
BLT	Bond line thickness
R_b	Thermal boundary resistance
R_c	Contact resistance of TIM
DF	Density factor
R_{jc}	Junction to case thermal resistance
K	Consistency index in (5)
r	Radius of the substrate
C	Empirical constant in (7)
R_{bulk}	Bulk thermal resistance
E_a	Activation energy
A	Acceleration factor
G	Shear modulus
G'	Storage shear modulus
G''	Loss shear modulus

Greek

σ	Surface roughness
Ψ_{J-a}	Junction to ambient thermal resistance
Ψ_{cs}	Case to sink thermal resistance
Ψ_{sa}	Sink to ambient thermal resistance
ϕ	Volume fraction of particles in TIMs
α	Biot number
τ_y	Yield stress of the TIM

I. INTRODUCTION

It is well known [1], [2] that when two solid surfaces are joined, as shown in Fig. 1(a) asperities on each of the surfaces limit the actual contact between the two solids to a very small fraction, perhaps just 1%–2% of the apparent

Manuscript received February 25, 2005; revised February 3, 2006.
The author is with Intel Corp., Chandler, AZ 85226-3699 USA and also with the Department of Mechanical and Aerospace Engineering, Arizona State University, Tempe, AZ 85287-6106 USA (e-mail: ravi.s.prasher@intel.com).
Digital Object Identifier: 10.1109/JPROC.2006.879796

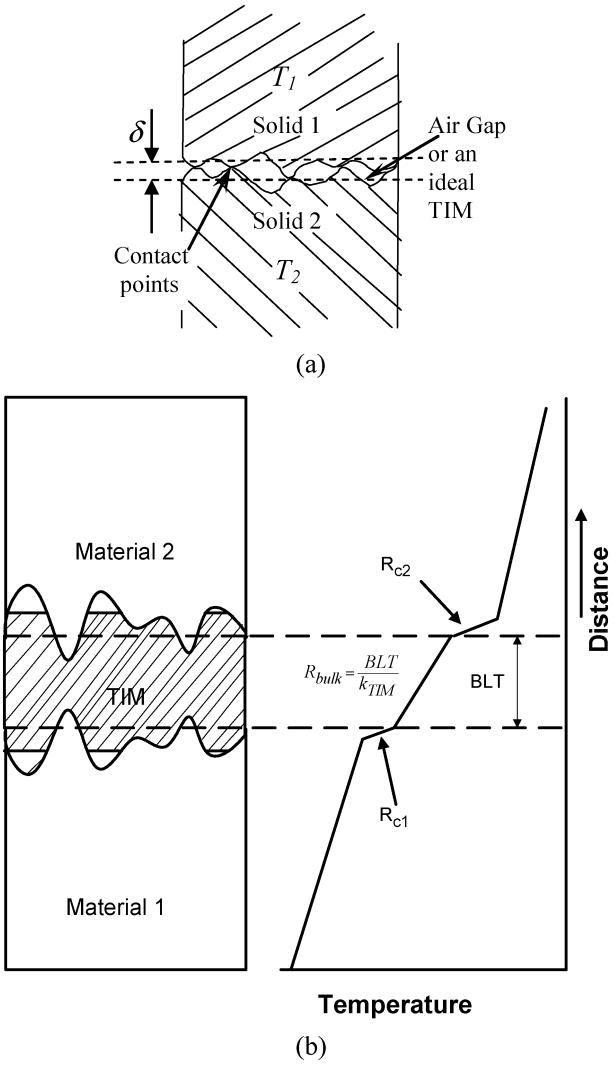

Fig. 1. *(a) Schematic showing that real area of contact is less than apparent area of contact. This figure also shows an ideal TIM, which completely fills the gap with zero thickness. (b) Schematic representing a real TIM.*

area for lightly loaded interfaces. Consequently, the flow of heat across such an interface involves solid-to-solid conduction in the area of actual contact A_c and conduction through the fluid occupying the noncontact area A_{nc} of the interface. This constriction of heat flow is manifested as thermal contact resistance (R_c) at the interface. The solid–solid contact resistance (R_{cs}) between two nominally flat surfaces 1 and 2 assuming plastic deformation of the asperities is given by [1]

$$R_{cs} = \frac{0.8\sigma}{mk_h}\left(\frac{H}{P}\right)^{0.95} \quad (1)$$

where $\sigma = (\sigma_1^2 + \sigma_2^2)^{0.5}$, σ is the root mean square roughness, $m = (m_1^2 + m_2^2)^{0.5}$, m = mean asperity slope, H the microhardness of the softer material, P the applied pressure, and $k_h = 2k_1k_2/(k_1 + k_2)$ is the harmonic mean thermal conductivity of the interface. m is a measure of the slope of the rough surface. m is given by, $m = \tan(\theta)$, where θ is the slope of the rough surface. Fig. 2 shows the variation of R_{cs} between copper and silicon for pressure range applicable to electronics cooling (5–150 psi). H of copper, which is the softer material is taken as 1280 MPa [3]. In Fig. 2, σ of the Cu is assumed 1 μm and σ of the Si is assumed 0.1 μm (assuming polished Si). m is calculated by the relation $m = 0.076(\sigma \times 10^6)^{0.5}$ [4]. Equation (1) neglects the contribution through the air trapped at the interface as shown in Fig. 1(a). The low pressure range is applicable in non-cpu products or for a heat sink on top of a large heat spreader as shown in Fig. 3(b). Fig. 2 shows that R_{cs} is very high at low pressures. Equation (1) is the best case result because it assumes plastic deformation of interfaces at all pressures and it assumes nominally flat surfaces. Fig. 3 shows two typical packaging architectures used in electronics cooling. Fig. 3 shows that the Si die or the chip is flat. In reality, the Si die or the chip surface is not flat. The chip is typically warped due to the coefficient of thermal expansion (CTE) mismatch between the die and the package substrate. A schematic of a warped chip is shown in Fig. 4. Warpage of the die for a flip chip package was measured by Verma *et al.* [5] and their results showed that depending on the temperature, the die surface could be very convex. The magnitude of the warpage depends on various factors such as geometry of the substrate, CTE mismatch between the substrate and the die, and the temperature. Due to the warpage of the die, the apparent area of the contact will be less as compared to a nominally flat die. This adds more resistance, thereby increasing R_c [2] as compared to that calculated from (1).

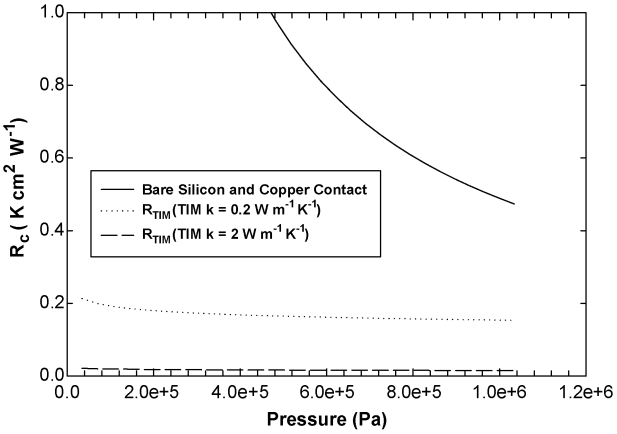

Fig. 2. *Thermal resistance without TIM and in presence of ideal TIM.*

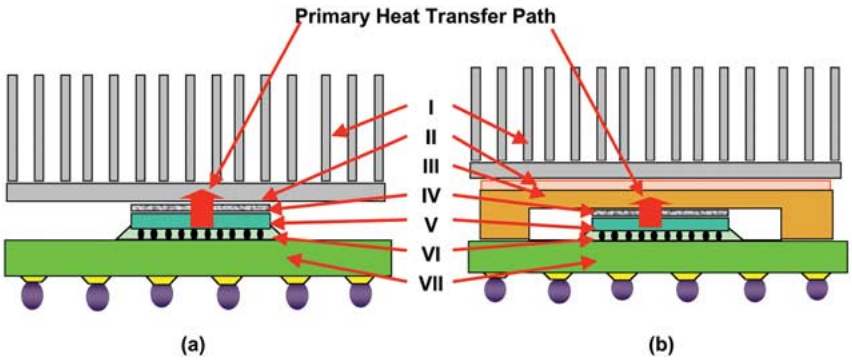

Fig. 3. *Schematic illustration of the two thermal architectures. (a) Architecture I, typically used in laptop applications. (b) Architecture II, typically used in desktop and server applications. I—heat sink; II—TIM; III—IHS; IV—TIM; V—die; VI—underfill; and VII—package substrate.*

To reduce R_c, the interfacial gap between the asperities in Fig. 1(a) has to be replaced by some highly conducting material. These materials are typically referred as thermal interface materials (TIMs). For the ideal case where the entire gap is filled by some TIM as shown in Fig. 1(a) analytical results are available [1]. R_c due to an ideal TIM (R_{cTIM}) for nominally flat surfaces can be calculated as [1]

$$R_{cTIM} = \frac{1.53\sigma}{k_{TIM}}\left(\frac{H}{P}\right)^{0.097} \tag{2}$$

where k_{TIM} is the thermal conductivity of the TIM. Fig. 2 also shows R_{cTIM} for two values of k_{TIM}. Fig. 2 shows that even for $k_{TIM} = 0.2$ W m^{-1} K^{-1} (typical value for pure polymers), R_{cTIM} is very small compared to R_{cs}. The total R_c is given by $R_{cTotal} = R_{cTIM}R_{cs}/(R_{cTIM} + R_{cs})$ because these resistances are in parallel. Fig. 2 shows that if it is possible to achieve the ideal TIM, R_c can be considerably lower; however, in reality it is not possible to achieve the ideal TIM due to various reasons. Real TIMs looks like that shown in Fig. 1(b). This figure shows that real TIMs have finite BLT, and at the interface they do not completely fill the voids because of their inability to completely wet the surface. Therefore, the thermal performance of real TIMs fall short of that predicted by (2). Equation (2) can be used for the best performance estimate of TIM performance.

From Fig. 1(b) it can be inferred that the total thermal resistance (R_{TIM}) of real TIMs can be written as [6]

$$R_{TIM} = \frac{BLT}{k_{TIM}} + R_{c1} + R_{c2} \tag{3}$$

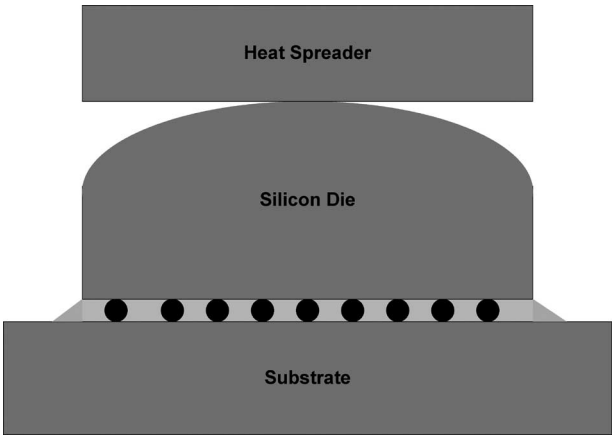

Fig. 4. *Schematic showing a warped die (not to scale). This schematic also shows that if there is no compliant TIM between the die and the heat spreader, then thermal linkage between the die and the substrate will be greatly reduced.*

where R_c represents the contact resistances of the TIM with the two bounding surfaces. In real electronics cooling applications, there are typically two packaging architectures used as shown in Fig. 3. In recent years there has been a great drive in the industry in reducing R_{TIM} primarily due to one very important reason. The projections for heat generation from the chip indicate that both the total power (Q) and the heat flux (q) are going to increase [7]. The heat flux from the chip is also nonuniform because both the core and cache are on the same die [8], [9]. More than 90% of Q is dissipated from the core, i.e., from a much smaller area of the chip. Even within the core, q is nonuniform. Readers are referred to the paper by Mahajan *et al.* [8] which appeared in the same issue of the transactions on the details of nonuniform heat fluxes from the die. The thermal problem for chip cooling is not about maintaining the average temperature of the chip below a design point, but it is about maintaining the

temperature of the hottest spot below a certain design point. Therefore, the thermal problem near the chip is very severe. Total thermal resistance for this situation can be written as [10]

$$\psi_{j-a} = DF \times R_{jc} + \psi_{cs} + \psi_{sa} \tag{4}$$

where ψ_{j-a} is the junction to ambient thermal resistance, R_{jc} is the junction to case thermal impedance for a uniformly heated die, ψ_{cs} is the case to sink resistance, and ψ_{sa} is the sink to ambient thermal resistance. DF in (4) is a factor that accounts for the nonuniformity of q and the die size [10]. The unit of DF is cm^{-2}. For a 1-cm^2 uniformly heated chip, DF = 1. Typically, DF will be greater than 1 due to nonuniformity of q. Equation (4) shows that any reduction in R_{jc} is multiplied by a factor greater than 1. Therefore, reduction in R_{jc} leads to a greater reduction in ψ_{j-a}. Note that R_{jc} is referred as thermal resistance in the paper, although the unit of R_{jc} is that for impedance. This is a common practice in the contact resistance community. Since R_{jc} is primarily due to TIM resistance, this has lead to a great drive in the electronics cooling industry to reduce the interface resistance.

In this review, the focus is mainly on polymeric TIMs due to their widespread use [11], [12]. Typically, these polymeric TIMs are filled with highly conducting particles to enhance their k. This paper is divided into seven sections including the introduction. Section II provides literature review on previous work done before the year 2000. Section III is devoted to the current state of fundamental knowledge and physics of TIMs. Reliability performance of polymeric TIMs is discussed in Section IV. Solder-based TIMs are briefly discussed in Section V. Implications of nanotechnology for TIM technologies are discussed in Section VI. Section VII highlights some of the key fundamental issues that need to be addressed in the future.

In the following, p denotes the particle, m the matrix, R_b the interface resistance between the particle and the matrix, d the diameter, k the thermal conductivity, and ϕ the volume fraction of the particles in the paper.

II. LITERATURE REVIEW

Almost all the work before the year 2000 in the area of TIMs was mainly experimental [13]–[20]. There was virtually no emphasis on any type of physics-based modeling of the thermal performance of TIMs. Some of very early work on thermal greases were performed for spacecraft applications [13], [14]. A great amount of experimental work were done by Fletcher and coworkers [15]–[19] between 1990 and 2000. Fletcher [16] published a review paper on different types of TIMs, which included metallic foils and polymeric TIMs. Mirmira *et al.* [17] evaluated various types of adhesives and correlated their data with an empirical model. Mirmira *et al.* [18] also published experimental evaluation of elastomeric TIMs. Marotta and Fletcher [15] performed experiments on different types of polymeric materials and compared their results with the plastic deformation model given by (1). Plastic deformation model given by (1) did not match well with their data. Marotta and Han [19] provided experimental data on different types of polymeric TIMs. Xu *et al.* [20] fabricated various sodium silicate based TIMs filled with boron nitride particles. In all these studies, there were no attempts made to separate the contact resistance and the bulk resistance of the TIMs. It is not possible to extract any type of design rules from any of these studies.

III. CURRENT STATUS

Equation (3) shows that to accurately model and understand the physics of TIM performance, three factors are to be modeled and understood: 1) k_{TIM}; 2) BLT; and 3) R_c. Reduction of R_{TIM} can be accomplished by reducing the BLT, increasing the thermal conductivity and reducing the contact resistances R_{c1} and R_{c2}. Table 1 shows the characteristics of some of the typical TIMs [11] and their advantages and disadvantages.

Since these TIMs are loaded with solid particles, the physics becomes complicated. First attempt to separate the bulk resistance (R_{bulk}) and R_c was made by the author [6], where he presented the physical model of the TIM as shown in Fig. 1(b). Since then there have been many studies in modeling of TIM performance. After 2000, many studies were performed to understand the thermal performance of various polymeric TIMs [21]–[31].

Fuller and Marotta introduced [22] a model for R_c of elastomeric materials; however, they did not have any model for the BLT of particle-filled elastomers. Their model for R_c matched well with data. The author and coworkers in a series of papers [6], [23]–[27] have introduced various models for BLT, k_{TIM}, and R_c. Their focus was mainly on grease, gel, and phase change materials (PCMs), as these materials are most widely used TIMs as compared to elastomers [11]. Goodson's group [21], [29], [30] has also performed modeling and experimentation of R_{TIM} and R_c. In this section modeling of k_{TIM}, BLT and R_c of different types of TIMs are discussed sequentially.

A. Thermal Conductivity (k_{TIM})

Polymeric TIMs are filled with highly conducting particles to increase k_{TIM}. Therefore, these TIMs can be treated as composites. Past literature is rife with modeling of thermal conductivity of composites (k_c) [32]–[39]; however, recently percolation phenomenon based modeling has been proposed to model k_{TIM} due to large contrast

Table 1 Summary of Characteristics of Some Typical TIMs

TIM Type	Thermal resistance of fresh samples ($^{o}C\ cm^{2}\ W^{-1}$) [68]	General Characteristics	Advantages	Disadvantages
Greases	0.1	Typically Silicone based matrix loaded with particles to enhance thermal conductivity	• High bulk thermal conductivity • Thin BLT with minimal attach pressure • Low viscosity enables matrix material to easily fill surface crevices • TIM curing not required • TIM Delamination is not a concern	• Susceptible to grease pump-out and phase separation • Considered messy in a manufacturing environment due to a tendency to migrate
Phase Change Materials	0.1	Polyolefin, epoxy, low molecular weight polyesters, acrylics typically with BN, or Al_2O_3 fillers	• Higher viscosity leads to increased stability and hence less susceptible to pump-out • Application and handling is easier compared to greases • No cure required • Delamination is not a concern	• Lower thermal conductivity than greases • Surface resistance can be greater than greases. Can be reduced by thermal pre-treatment • Requires attach pressure to increase thermal effectiveness hence can lead to increased mechanical stresses
Gels	0.08	Al, Al_2O_3, Ag particles in silicone, olefin matrices that require curing	• Conforms to surface irregularity before cure • No pump out or migration concerns	• Cure process needed • Lower thermal conductivity than grease • Lower adhesion than adhesives; delamination can be a concern
Adhesives	Data not available	Typically Ag particles in a cured epoxy matrix	• Conform to surface irregularity before cure • No pump out	• Cure process needed • Delamination post reliability testing is a concern
			• No migration	• Since cured epoxies have high post cure modulus, CTE mismatch induced stress is a concern

Table 2 Various Models to Predict the Thermal Conductivity of Particle-Laden TIMs

Name of the Model	Formula	Remarks	Source
Maxwell-Garnett with R_b	$\frac{k_c}{k_m}=\frac{[k_p(1+2\alpha)+2k_m]+2\phi[k_p(1-\alpha)-k_m]}{[k_p(1+2\alpha)+2k_m]-\phi[k_p(1-\alpha)-k_m]}$ $\alpha=\frac{2R_bk_m}{d}$ $\frac{k_c}{k_m}=\frac{(1+2\alpha)+2\phi(1-\alpha)}{(1+2\alpha)-\phi(1-\alpha)}$ for $k_p >> k_m$	Spherical particles Typically valid for $\phi < 0.4$	32, 33, 34, 35
Bruggeman symmetric model	$(1-\phi)\frac{k_m-k_c}{k_m+2k_c}+\phi\frac{k_p-k_c}{k_p+2k_c}=0$ (R_b not included)	Spherical particles Typically good at higher ϕ	36, 42
Bruggeman asymmetric model with R_b	$(1-\phi)^3=\left(\frac{k_m}{k_c}\right)^{(1+2\alpha)/(1-\alpha)}\times\left\{\frac{k_c-k_p(1-\alpha)}{k_m-k_p(1-\alpha)}\right\}^{3/(1-\alpha)}$ $\frac{k_c}{k_m}=\frac{1}{(1-\phi)^{3(1-\alpha)/(1+2\alpha)}}$ for $k_p >> k_m$	Spherical particle	37, 42
Percolation model	$k_c=k_p(\phi-\phi_p)^2$ valid only for $k_p >> k_m$	Cubical particles	41, 42, 43, 44, 45, 46, 47, 48
Percolation model with R_b	Numerical	Cubical particles	49,50
Numerical model with R_b	Resistive network model	Any type of particles	38, 39

k_m = thermal conductivity of matrix, k_p = thermal conductivity of particles, R_b = interface resistance between particles and the matrix, ϕ = volume fraction of the particles.

in the thermal conductivity of the particles and the polymer matrix [40]. Percolation modeling [41] will be discussed in some details later. Table 2 lists some of the most common and important analytical models along with percolation model and sources of numerical models. The focus in this review is on spherical particles; however, some of the references given in this paper have also dealt with two-dimensional systems such as aligned cylindrical particles [32], [34], [38], [39]. The Maxwell–Garnett (MG) effective medium model can be considered a good model for low volume fraction (< 40%). Therefore, MG is not used in modeling k_{TIM}, as commercial TIMs are loaded in excess of 60% with conductive particles.

For high volume fraction, Bruggeman symmetric model (BSM) has been used to predict the electrical conductivity of composites [42]. Limited used of BSM has been made in predicting thermal conductivity [43]. One of the biggest drawbacks of BSM is that it does not include the interface resistance between the particle and the matrix, which will be shown later to be very important. The interface resistance between the particle and the matrix is denoted as R_b; however, the strength of BSM is that it predicts a percolation threshold in the limit of infinite contrast in the conductivity of the particle and the matrix [42]. Other analytical models given in Table 2 do not predict percolation threshold.

There is another model due to Burggeman, which is known as the Burggeman asymmetric model (BAM) [42]. Every *et al.* [37] modified the BAM to include R_b between the particle and the matrix. This model is capable of predicting thermal conductivity of spherical particles for larger volume fractions.

Recently Devpura *et al.* [40] proposed the use of percolation model for TIMs due to large contrast in the conductivities of the particles and the polymer matrix. Liang *et al.* [44] and Liang and Ji [45] used the percolation model to predict the thermal conductivity of thin composites. Percolation is a geometrical phenomenon. It basically means that after some volume fraction, called the percolation threshold (ϕ_c), there is a continuous path for heat conduction trough the particles because the conducting particles start to touch each other as shown in Fig. 5(a). The percolation model as given in Table 2 is strictly valid only near the percolation threshold. There are some very important subtle points that have been overlooked in applying the percolation-based models to predict thermal conductivity of composites [40], [44], [45]. The percolation phenomenon is strictly valid for $k_p/k_m \rightarrow \infty$. This is possible in reality for electrical conductivity as perfect insulators are possible. For thermal conductivity, this is not possible in reality because for any solid there is a nonzero thermal conductivity. The percolation model was numerically evaluated [41] for planar geometries such as cubical particle. The percolation threshold for cubical particles (p_c) is given in Table 3 for different arrangements of particles. Zallen [46] used p_c and the maximum packaging fraction for spherical particles to obtain ϕ_c for spherical particles, which is around 15% for all arrangements of particles as shown in Table 3. For two-dimensional composites made from aligned cylinders, ϕ_c is 0.45 [46]. If $k_p/k_m \rightarrow \infty$ then this scaling is all right and the percolation model can be used for spherical models; however, if $k_p/k_m \neq \infty$, then there is a problem with spherical particles. For cubical particles, if $k_p/k_m \neq \infty$ but if the ratio is still very large, a correction to the percolation model has been proposed [47]. For spherical particles due to the curvature of the surface, there will be constriction and spreading of heat flow lines near the particle and matrix interface. This constriction/spreading of heat flow lines is not taken into consideration in the percolation model. This effect will increase with decreasing contrast between k_p and k_m. This was recently shown by Ganpathy *et al.* [39]. This is not a problem for planar geometry. Ganpathy *et al.* [39] also showed that for $k_p/k_m = \infty$ nonplanar results reduce to the planar results which means that percolation model could strictly be used for spherical particles only in the limit of $k_p/k_m = \infty$. Therefore, percolation model has been successful in the prediction of electrical conductivity of composites made from spherical particles [48] and other nonplanar geometries [49]. Various modifications to the percolation model has also been proposed [48]. The percolation model for $k_p/k_m \rightarrow \infty$ can also be used to capture thin-film effects [50] which happens when the thickness of the composite is comparable to the dimensions of the particles. Recently Devpura *et al.* [51] and Keblinski and Cleri [52] considered the percolation model in the presence of R_b and showed that percolation phenomenon is diminished in the presence of R_b. The percolation model has been applied with some success in predicting the thermal conductivity of superconductors [53] and some complicated compounds [54].

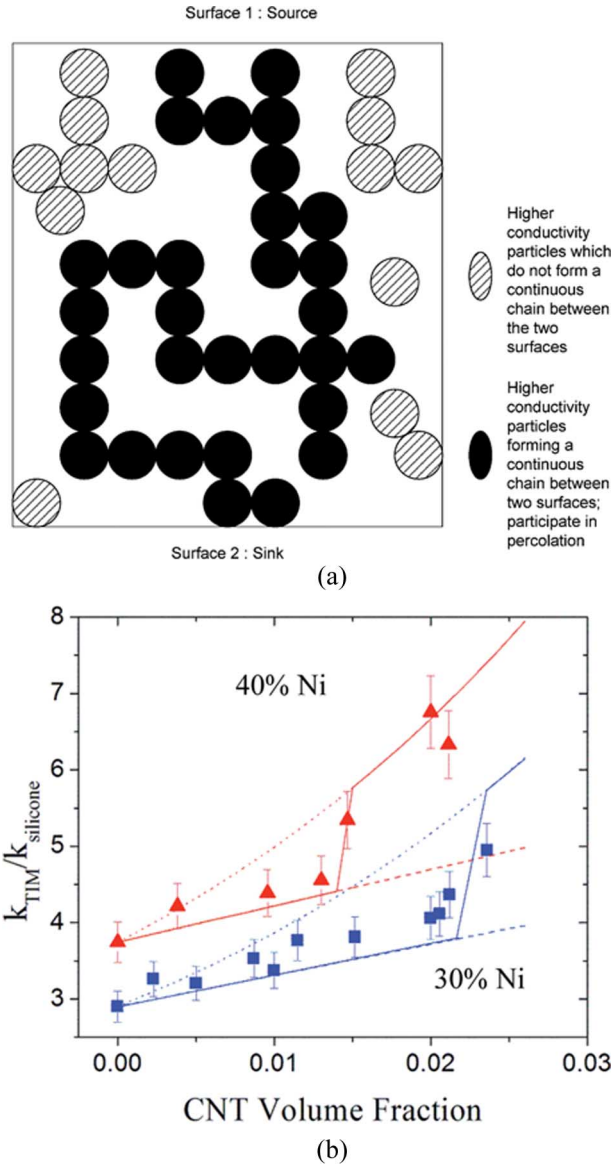

Fig. 5. *(a) The phenomenon of site percolation occurring with the formation of a continuous chain between the two surfaces by the highly conducting particles. (b) Thermal conductivity of TIM made from CNT and Ni particles (Hu et al. [29]). This figure indicates the presence of percolation. Solid and dashed lines are model developed by Hu et al. [29] based on bond percolation. This figure shows a jump in thermal conductivity near percolation threshold, which means that the CNT is making contacts with different Ni particles.*

Table 3 Critical Concentrations for Site Percolation on a Variety of Lattices (Zallen [46]). p_c is for Cubical Particles and ϕ_c Is for Spherical Particles. fcc: Face Centered Cubic, bcc: Body Centered Cubic, sc: Simple Cubic, rcp: Random Close Packing

Lattice or structure	p_c	ϕ_c
fcc	0.198	0.147
bcc	0.245	0.167
sc	0.311	0.163
Diamond	0.328	0.146
rcp	0.28	0.16

All the discussions on the percolation model given in the previous paragraph is for site percolation. There is another type of percolation known as bond percolation, which is applicable to fiber-type particles [41]. Hu *et al.* [29] applied a bond percolation model to a TIM made from carbon nanotube (CNT) and Ni particles. Their data and model predictions are shown in Fig. 5(b). Fig. 5(b) shows the existence of a percolation threshold at a very small volume fraction of CNT. Their work indicates the potential of using CNTs in TIMs.

Thermal conductivity of composites can also be calculated using computationally intensive numerical methods and there are plenty of literature on that (see [38] and [39] for details). Recently Ganpathy *et al.* [39] proposed a numerical model for nonplanar geometry, which uses MG model to define the thermal conductivity of a unit cell. This transformation converts the nonplanar geometry to a planar geometry while capturing the effects of constriction/spreading of heat flow lines due to nonplanar geometry. This model reduces the number of elements in finite element modeling by a huge amount. Their model also includes R_b and it compared very well with experimental data. For complicated situations such as misaligned fibers or short fibers, some literature exists [34], [55]. Progelhof *et al.* [56] have also provided a detailed discussion on various models of thermal conductivity of composites.

Recently the author used the BAM to model k_{TIM}. Fig. 6 shows the comparison between experimental data on k_{TIM} from various sources and BAM. Fig. 6 shows that BAM is very successful in modeling k_{TIM}. Data from He [57], [58] for silicone-based TIMs was given in terms of weight fraction. To obtain the volume fraction silicone oil density was assumed to be 971 kg m^{-3} [59]. Fig. 6 shows that the importance of R_b. BAM match the data assuming $\alpha = 0.1$ where α is the Biot number. Assuming $k_m = 0.2$ W m^{-1} K^{-1} and diameter (d) of the particles 10 μm (typical in commercial TIMs), $\alpha = 0.1$ gives $R_b = 5 \times 10^{-6}$ K m^2 W^{-1}. R_b at the interface between the particle and the matrix could arise due to two factors: 1) phonon acoustic mismatch and 2) incomplete wetting of the interface by the polymer. R_b due to phonon acoustic mismatch is of the order of 10^{-8} K m^2 W^{-1} [61] at room temperatures. This means that $\alpha = 0.0002$ due to phonon acoustic mismatch for $d = 10$ μm and $k_m = 0.2$ W m^{-1} K^{-1}. Prasher *et al.* [61] recently showed that at room temperature phonon acoustic mismatch could be ignored in comparison to the incomplete wetting; however, for nanoparticles phonon acoustic mismatch could become important. R_b due to incomplete wetting of the particle could become a function of the volume fraction because it is difficult to completely wet the surfaces with increasing volume fraction due to difficulty in processing conditions. The percolation model and BSM will predict much higher conductivity than the experimental data. Fig. 6 also shows the inability of MG model in predicting k_{TIM} for higher volume fractions. Data on some particle filled mold compounds by Bujard *et al.* [62], [63] also show that at volume fractions as high as 80% the thermal conductivity was only around 4.5 W m^{-1} K^{-1}. BAM is much simpler to use than any numerical model. BAM is a model, which takes the closeness of the particles

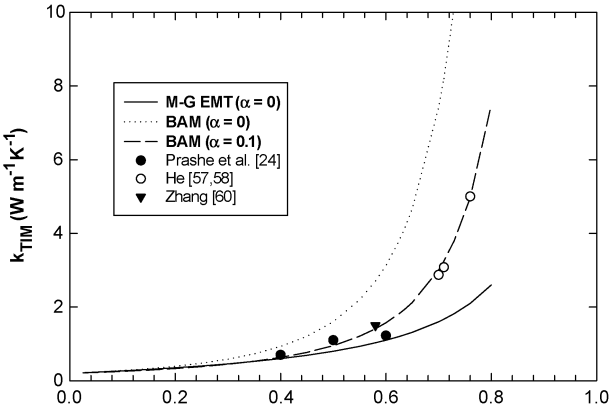

Fig. 6. *Comparison of Bruggeman Asymmetric model with experimental data.*

into account while accounting for R_b whereas MG does not take the closeness of the particles into account.

B. BLT: Rheological Modeling

The first serious effort to model the BLT was made by Zhou and Goodson [21]; however, they treated particle-laden polymeric (PLP) TIMs as Newtonian fluids. This led to the unphysical conclusion of BLT = 0 for larger time (t). Prasher *et al.* [23], [25] measured the viscosity of various silicone-based PLT TIMs and showed that these TIMs behave as Herschel–Bulkley (H–B) fluid. The viscosity (η) for H–B fluid is given by [64]

$$\eta = \frac{\tau_y}{\dot{\gamma}} + K(\dot{\gamma})^{n-1} \tag{5}$$

where τ_y is the yield stress of the polymer, $\dot{\gamma}$ is the strain rate, K the consistency index, and n is an empirical constant. Prasher *et al.* [25] showed that steady state BLT depends only on τ_y. Fig. 7 shows τ_y for three different PLP TIMs loaded with different volume fractions of particles. Fig. 7 shows that τ_y increases with increasing volume fraction of the particle. Applying the law of conservation of momentum and mass, the BLT by using (5) is given by

$$\text{BLT} = \frac{2}{3} r \left(\frac{\tau_y}{P}\right) \tag{6}$$

where r is the radius of the substrate and P the applied pressure. Prasher *et al.* [26] showed that (6) under predicted the BLT by a huge margin. They introduced an empirical model

$$h_L = C\left(\frac{\tau_y}{P}\right)^m \tag{7}$$

where C and m are empirical constants. They found $m = 0.166$ and $C = 0.31 \times 10^{-4}$. Subsequently the author [26] offered an explanation for the empirical (7) by applying finite size scaling argument to a percolating system of particles. A heterogeneous system can be macroscopically treated, as homogenous only if the thickness (BLT in this case) is much larger than the diameter of the particles. At high pressures the BLT of TIMs range from 20 to 50 μm. If the particle diameter is of the order of 10 μm, then the TIM cannot be treated a macroscopically homogeneous system. Prasher [26] used the finite size scaling of elasticity modulus [65] for a thin percolating systems as a clue to scale τ_y of the PLT TIM. Prasher [26] also considered the fact that if BLT $\gg d$ (at low pressures) then any BLT model should reduce to (6). Based on these arguments Prasher's model [called the scaling-bulk (S-B) model] is given as

$$\text{BLT} = \frac{2}{3} r \left[c\left(\frac{d}{\text{BLT}}\right)^{4.3} + 1 \right] \left(\frac{\tau_y}{P}\right) \tag{8}$$

where $c = 13708$. This equation at high pressures shows that $m = 0.188$ which is very close to the m obtained in the empirical (7). Equation (8) reduces to (6) for a very small value of P/τ_y and to (7) for a large value of P/τ_y with $m = 0.188$. The author also proposed an approximate version of (8) for quick calculations. This is given as

$$h_L = \frac{2r}{3}\left(\frac{\tau_y}{P}\right) + \left(\frac{cr}{1.5}\right)^{0.188} d^{0.811} \times \left(\frac{\tau_y}{P}\right)^{0.188}. \tag{9}$$

Fig. 8 shows the comparison of (9) (S-B model) with experimental data obtained on various PLT TIMs [25]. The author also compared (8) with a variety of other suspensions for d as large as 80 μm and as small as 2 μm and showed that (8) matches very well with the data.

Recently Hu *et al.* [30] proposed a model based on the percolation phenomenon for BLT. Their model assumes that the force applied is supported by the fluid (polymer) and the particles separately. They calculated the force carried by the particles by applying percolation model and assuming that BLT is less than the correlation length. An empirical constant (c_f) was used to calculate the force carried by the particles. For the force carried by the liquid, they treated the systems as a Newtonian liquid. Their

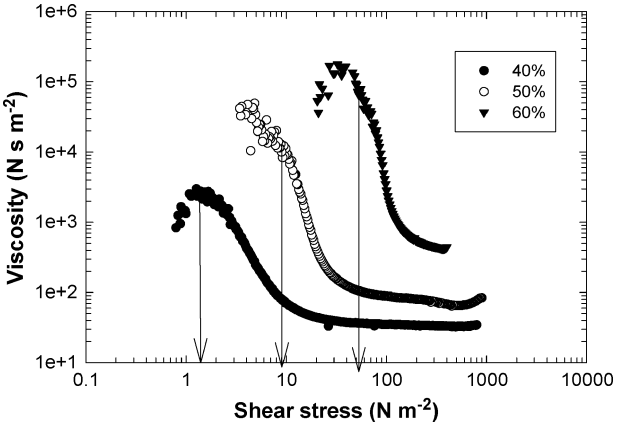

Fig. 7. *Viscosity versus shear stress to obtain yield stress for different volume fraction of particles in silicon-based greases [25].*

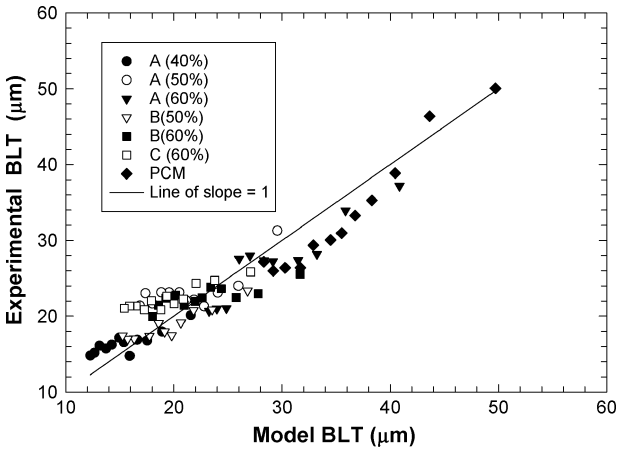

Fig. 8. *Comparison of scaling bulk model with experimental data for the PCM [25], [26].*

prediction leads to conclusion that BLT $\propto P^{-0.5}$ whereas data by Prasher *et al.* [25] show much smaller dependence on P. It is also not clear if c_f is a universal constant or it depends on TIM type.

Equation (8) can be used for PCM, greases, and precure gels, as these TIMs are well described by the H–B model. Equation (8) cannot be used for elastomeric TIMs or cured gels. The author is not aware of any systematic study of BLT for PLP elastomeric TIMs. Fuller and Marotta [22] conducted a study on pure polymers and metal joints; however, they measured BLT from experiments and their focus was solely on R_c. Modeling of BLT for PLP elastomers could be handled by using the approaches by Lewis and Nielsen [66] or by applying the percolation models for the elastic properties of composites [65]. The use of elastomeric TIMs is very limited in current technologies because of their poor thermal performance as compared to greases, gels, and PCMs [11], [68]. Therefore, in the opinion of the author, much advancement in the modeling of BLT of PLP elastomers is not expected in the future.

C. Dependence of Bulk Thermal Resistance on Particle Volume Fraction

The bulk thermal resistance of the TIM is given by

$$R_{\text{bulk}} = \frac{\text{BLT}}{k_{\text{TIM}}}. \tag{10}$$

Using (7), R_{bulk} can be written as

$$R_{\text{bulk}} = \frac{1}{k_{\text{TIM}}} C \left(\frac{\tau_y}{p}\right)^m \tag{11}$$

τ_y depends on particle volume fraction (ϕ) as shown by Fig. 7. If electrostatic interaction [64] is assumed to be negligible compared to the Van der Walls interaction in the particle-laden polymer, then τ_y can be expressed as [64]

$$\tau_y = A\left[\frac{1}{(\phi_m/\phi)^{1/3} - 1}\right]^2 \tag{12}$$

where A is constant and ϕ_m is the maximum particle volume fraction. Equation (12) can also be written as

$$\tau' = \frac{\tau_y}{A} = \left[\frac{1}{(\phi_m/\phi)^{1/3} - 1}\right]^2 \tag{13}$$

where τ' is the dimensionless yield stress. Using τ', (11) can be written as

$$\frac{R_{\text{bulk}} p^m}{C A^m} = \frac{\tau'^m}{k_{\text{TIM}}}. \tag{14}$$

Using the BAM and (14), Prasher *et al.* [25] showed that R_{bulk} reaches a minima with respect to the volume fraction of the fillers. This was experimentally verified by them. Their result is shown in Fig. 9. Fig. 9 shows that there is an optimal volume fraction for the minimization of the thermal resistance. Prasher [26] recently performed parametric studies on the thermal resistance for various factors such as ϕ, diameter of the filler and the applied pressure. The key conclusion from Prasher's parametric study was that there is an optimal volume fraction for a

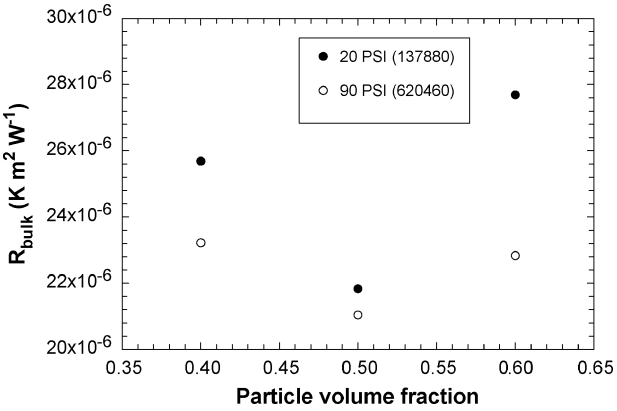

Fig. 9. *Experimental results for resistance versus particle volume fraction for silicon-based thermal greases [25].*

given pressure and filler shape, above which thermal resistance of the TIM increases.

D. Contact Resistance

Various authors [6], [21], [67] have modeled the contact resistance of PCM, grease, and uncured gel TIMs, assuming them to behave like a pure liquid. Some groups have considered incomplete wetting of the interface between the TIM and the substrate [6], [21] and other groups have considered complete wetting of the interface [67]. The author [6] proposed an incomplete wetting by applying surface chemistry. This model was based on the assumption that due to trapped gases in the valleys of the rough surface, the TIM is unable to fill all the valleys. This is shown in Fig. 10. By applying force balance which includes the externally applied pressure, capillary force due to the surface tension of the TIM and back pressure due to the trapped air, it was possible to calculate the penetration length of the TIM in the interface. The author defined a constriction resistance parameter based on A_{real} and A_{nominal} as shown in Fig. 10. For $k_{\text{TIM}} \ll k_{\text{substrate}}$ the surface chemistry model is given by

$$R_{c_{1+2}} = \left(\frac{\sigma_1 + \sigma_2}{2k_{\text{TIM}}}\right)\left(\frac{A_{\text{nominal}}}{A_{\text{real}}}\right) \tag{15}$$

where σ_1 and σ_2 are the surface roughness of the two substrates sandwiching the TIM. A_{real} can by calculated from penetration length of the TIM. The surface chemistry model was in good agreement with PCM and greases as shown in Fig. 11. This model was also used by Zhou and Goodson [21]. However, considering the later finding by the author [25], [26] that these TIMs posses yield stress and viscosity, which means that they are semisolid and semiliquid, the pure liquid-based surface chemistry model is not good enough for the modeling of the contact resistance of PLP TIMs. Intuitively speaking, the area

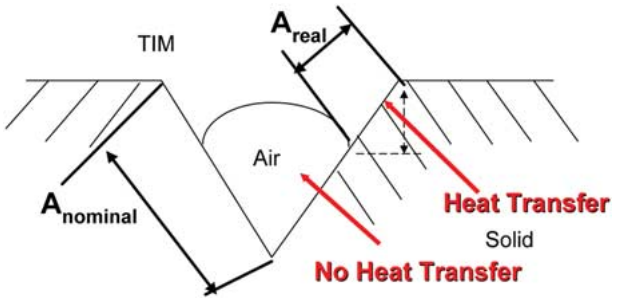

Fig. 10. *Mechanism of heat transfer near the TIM substrate interface [6].*

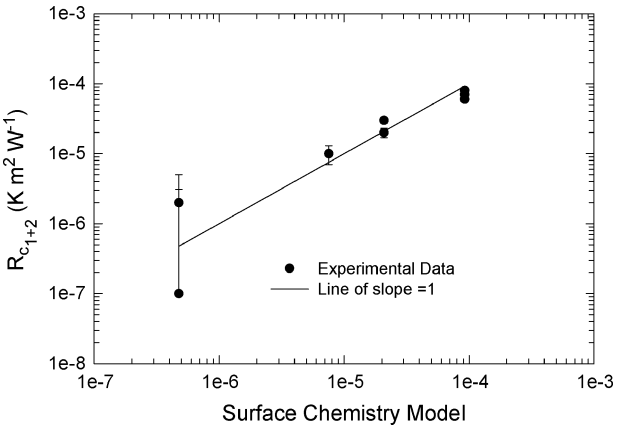

Fig. 11. *Comparison of the surface chemistry model with experimental results for PCMs [6].*

covered by the PLP in the valleys of the interface as shown Fig. 1 will eventually depend on the pressure and yield stress. This relation could be somewhat similar to that obtained for bare metallic contacts where the contact resistance depends on the pressure and the hardness of the softer material. For PLP TIMs most likely hardness will have to be replaced by the yield stress. Internal studies at Intel on various state-of-the-art TIMs have suggested, however, that bulk resistance of the TIM is more dominant than R_c.

For cured gels, Prasher and Matyabus [27] proposed a semiempirical model for R_c, which has similar form as (1). This model is given as

$$\frac{R_c\sigma}{k_{\text{TIM}}} = c\left(\frac{G}{P}\right)^n \tag{16}$$

where $G = \sqrt{G'^2 + G''^2}$. G' is the storage shear modulus and G'' is the loss shear modulus of the TIM. For cured gels, $G' > G''$, and for uncured gels, $G' < G''$. Note that uncured gels are nothing but greases. Fig. 12 shows the comparison between this model and experimental data on four different formulations of gels.

For the contact resistance of elastomers, Fuller and Morotta's [22] model can be used. Morrotta *et al.* [28] also applied their elastomer model to predict the R_c of TIMs made from graphite foils.

IV. RELIABILITY PERFORMANCE OF POLYMERIC TIMs

The focus of all the research on polymeric TIMs until now has been on understanding the behavior of freshly made samples. In reality, however, these TIMs are exposed to high temperatures and harsh conditions for a long period

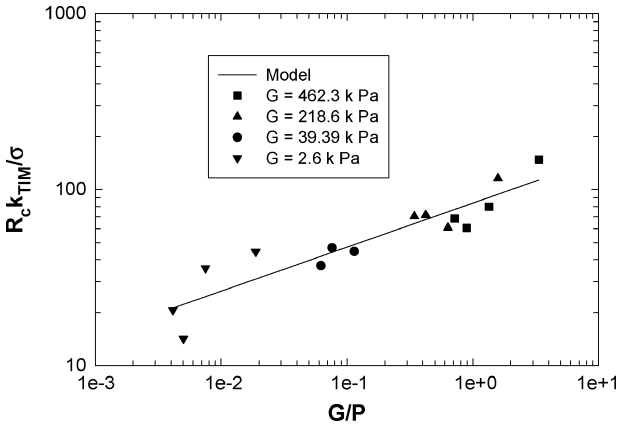

Fig. 12. $R_c k_{TIM}/\sigma$ ***versus G/P for gel TIM [27].***

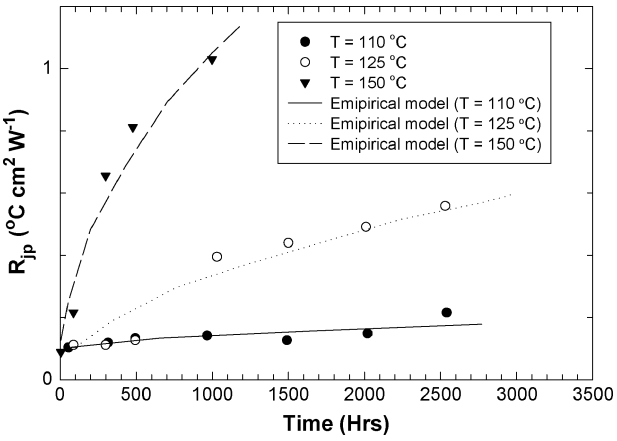

Fig. 14. ***Degradation of thermal resistance with time. Lines are the empirical curve fit of the form given by (17).***

of time. Assuming that a processor life is seven years, this translates into approximately 61 000 h under continuous operation or 35 000 h for 14 h a day. If the chip temperature is 100 °C, then the polymers in the TIM are being exposed to relatively high temperatures for a very long time. Polymers degrade under such high temperatures [69]. It is not possible to test these TIMs for such long times to understand their behavior for exposure to high temperatures. Therefore, to understand the degradation behavior accelerated life time testing is performed [68]. Under accelerated testing the TIM is exposed to higher temperatures than the use condition temperature. For example, if the chip temperature is 100 °C it could be tested at 125 °C and 150 °C for a much shorter period than the use condition. The thought behind this is that higher temperature will accelerate the degradation and engineers would be able to generate degradation models. Fig. 13 shows themogravitic analysis (TGA) of a PCM. Fig. 13 shows that polymer loses weight due to oxidation. With the current level of understanding, it is not possible to relate this behavior to degradation in the thermal performance of TIMs. Therefore, empirical methods are typically applied. Fig. 14 shows the thermal resistance (R_{jc}) of a PCM TIM as function of time and temperature. The lines represent an Arreheneous-type model. These lines are curve fit and their form is

$$R_{jc}(t) = R_{jc}(t=0) + A\sqrt{t}\exp\left(\frac{-E_a}{k_b T}\right) \qquad (17)$$

where E_a is the activation energy, A the acceleration factor, and k_b the Boltzmann constant. t represents the time and the first term on right-hand side is the R_{jc} at $t = 0$, i.e., R_{jc} of a pristine fresh sample which has not been exposed to high temperature. The focus of the research discussed in previous sections have been on $R_{jc}@t = 0$. Equation (17) shows some type of a diffusion process due to square root dependence on time [69]. Once A and E_a are known from matching the data at higher temperatures, the use temperature can be put into (17) to obtain the value of R_{jc} at the use temperature and end of life of the product. In the industry, TIMs are designed for end-of-life performance. Therefore, it is very possible and quite frequent that a particular TIM gives great $R_{jc}@t = 0$ performance, but that TIM might degrade so much that at end of life it gives very bad performance.

There is no mechanistic understanding of the degradation of the thermal performance of the TIMs due to large exposures to high temperatures. The form of (17) suggests some type of diffusion process; however, it is not clear what is really diffusing. Even if it is assumed that the oxidation of the TIMs follows a diffusion process, no

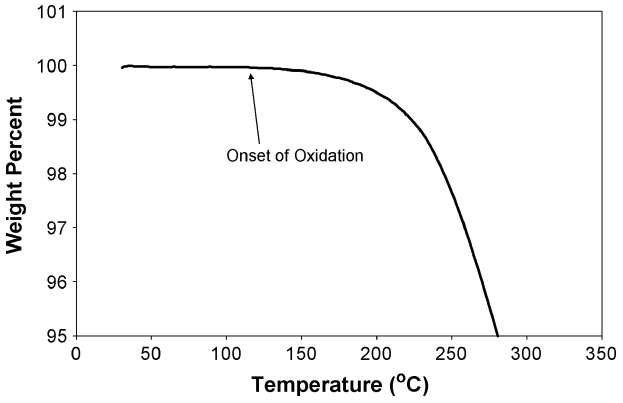

Fig. 13. ***Thermogravimetric analysis of a PCM showing onset of oxidation at about 125 °C.***

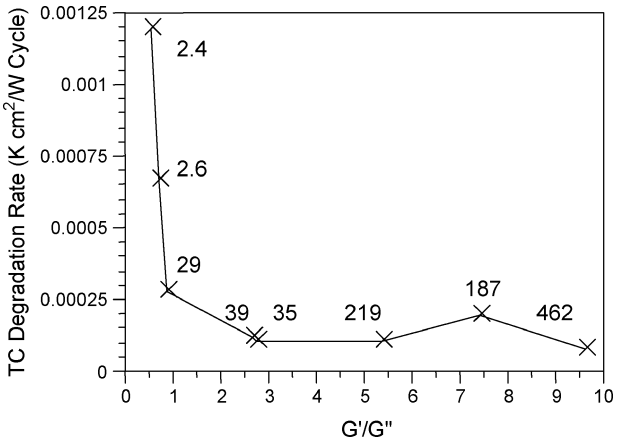

Fig. 15. *Effect of G'/G'' on the degradation rate, as measured by thermal performance of gel TIMs subjected to temperature cycling. The labels present the value of G for each sample [27].*

attempt has been made to relate this to thermal performance. This area of research is wide open.

Thermal greases suffer from another type of degradation, which commonly known as pump-out [11]. Pump-out typically happens in temperature or power cycling. Recently Prasher and Matyabus [27] related the pump out problem to the ratio of G' and G''. They showed that to avoid pump out G' of grease should be greater than G''. This is exactly what a gel does. Gel is nothing but a cured grease. Fig. 15 shows the rate of degradation of thermal performance versus G'/G''. Fig. 15 shows that the degradation rate is almost a constant after $G' > G''$.

Other types of stress testing include testing under humidity, temperature cycling, shock and vibration. For most of these stress, testing mechanistic understanding is still missing and most of the modeling and analysis are empirical in nature.

V. SOLDERS

Solders are now actively being pursued as TIMs due to their large thermal conductivity [70]–[72]. Chiu *et al.* [70] characterized various solder TIMs and showed that some solders possessed very small thermal resistance. Voiding is the biggest problems for solder. Pritchard *et al.* [71] performed numerical studies to understand the influence of voiding on the over all thermal performance of solders. Hu *et al.* [72] have performed experimental characterization of voids in solder type TIMs. Microscopic modeling of thermal performance of solders is missing from the literature primarily because of the lack of a driving force. In the opinion of the author, this is because: 1) most of the solders' performance is inherently very good and 2) they are not preferred over polymer TIMs because of cost and the complexity involved in implementing solder TIMs as compared to polymer TIMs.

VI. NANOTECHNOLOGY IN TIMs

Ever since it was demonstrated that CNTs [73] have very high thermal conductivity, various CNT-based composites have been proposed and evaluated [74]–[77]. Although promising candidates as fillers, CNTs have a big limitation. Due to their small diameter, the impact of any thermal interface resistance between the polymer and the CNTs on k_{TIM} will be huge. Huxtable *et al.* [78] have experimentally measured R_b between CNTs and various liquids and they have shown that R_b is substantial (8.33×10^{-8} K m^2 W^{-1}). Nan *et al.* [79] recently proposed simplified effective medium model to compute k of CNT-based composites. Hu *et al.* [29] have performed a feasibility of study of CNT-based TIM as mentioned earlier. Their preliminary results are encouraging and show the potential of achieving percolation threshold are very small volume fractions. Another potential problem of using CNT is that the BLT of the resultant TIM will be high because the yield stress of fiber-based composites are very high. Therefore, for a fair comparison between CNT-based TIMs and conventional TIMs thermal resistance is the right metric as compared to k_{TIM}.

Xu and Fisher [80], [81] have grown CNTs directly on the back of Si. Their concept is schematically shown in Fig. 16. The heat spreader was pressed against the as-grown CNTs. They have also used PCM TIM and as-grown CNT combination to reduce the thermal resistance. Hu *et al.* [82] have experimentally measure the thermal resistance for this concept and their results are shown in Fig. 17. At this time there is no physics-based model for this concept; however, it looks very promising. It seems that this concept will not suffer from the reliability problems of polymer-based TIMs as mentioned earlier, because this does not use polymers. It is more complex and expensive than polymer-based TIMs; however, it seems that this concept has good potential and this could lead to various creative ideas, such as those shown by Xu and Fisher [81], where they used PCM TIMs.

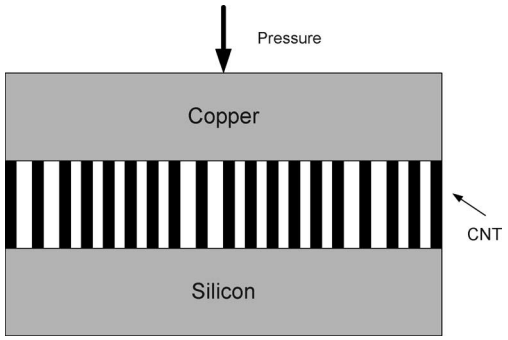

Fig. 16. *Schematic showing the use of CNT grown in the back of Si (Xu and Fisher [80], [81].*

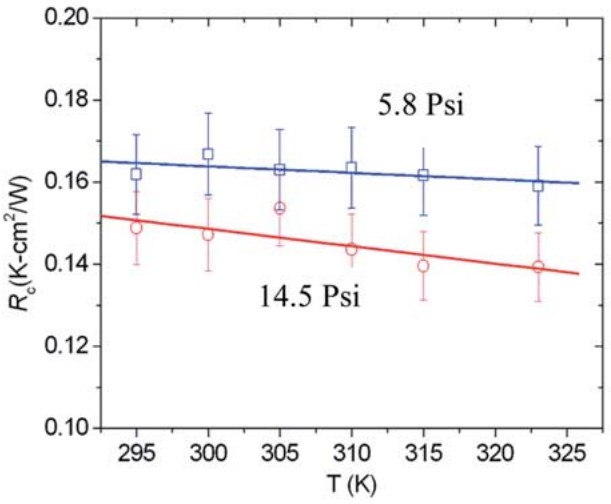

Fig. 17. *Thermal resistance of aligned CNT on Si. The other surface is copper (Hu et al. [82]).*

Researchers have also proposed the use of nanoparticles as fillers [83], [84]; however, nanoparticles suffer from the same problem as CNTs, i.e., R_b will play a dominant role in nanoparticle-based composites. Putnam *et al.* [85] measured R_b between polymer and alumina in the range 2.5×10^{-8} K m^2 W^{-1}–5×10^{-8} K m^2 W^{-1}. This means that the critical radius ($\alpha = 1$) below which the thermal conductivity of the nanocomposite is less than the conductivity of the matrix varies between 5 and 10 nm. The yield stress of particle-laden polymers increases with decreasing particle diameter [64]. Therefore, the BLT of these nanoparticle-based TIMs could also be higher than conventional TIMs. Therefore, at this time it is not clear if nanocomposites can really be of great use as TIMs.

VII. FUTURE DIRECTIONS

The focus of future research should be on understanding the reliability and performance degradation of TIMs. Current commercial TIMs are capable of providing a thermal resistance between 0.03 and 0.1 °C cm^2 W^{-1} for fresh samples [68]; however, due to degradation at large exposures to high temperatures as discussed earlier, the thermal performance can degrade severely depending on the temperature of the processor and time of exposure. There is no mechanistic understanding of these degradations. Fundamental physics-based modeling is needed to relate the degradation of the polymer properties to thermal properties of the polymer composites.

Use of nanoparticles and nanotubes is almost inevitable; however, any research in this areas should take the performance of the current commercially available TIMs as benchmark [68]. Research should also focus on minimizing the total thermal resistance rather than just increasing the thermal conductivity. Figs. 6 and 9 clearly show that although k_{TIM} increased with increasing volume fraction, bulk resistance reached a minima due to competing effects between the BLT and k_{TIM}.

A good physics-based model for the contact resistance between the particle-laden TIMs and the substrate is still lacking from the literature. Contact resistance will become important for thin highly conducting TIMs. Modeling of the CNT concept by Xu and Fisher [80], [81] will be also needed in the future due its promise as interface material. ■

REFERENCES

[1] M. M. Yovanovich and E. E. Marotta, "Thermal spreading and contact resistances," in *Heat Transfer Handbook*, A. Bejan and A. D. Kraus, Eds. Hoboken, New Jersey: Wiley, 2003, pp. 261–395.

[2] C. V. Madhusudana, *Thermal Contact Conductance*. New York: Springer-Veralag, 1996.

[3] A. Iwabuchi, T. Shimizu, Y. Yoshino, T. Abe, K. Katagiri, I. Nitta, and K. Sadamori, "The development of a vikers-type hardness tester for cryogenic temperatures down to 4.2 K," *Cryogenics*, vol. 36, no. 2, pp. 75–81, 1996.

[4] M. A. Lambert and L. S. Fletcher, "Thermal contact conductance of non-flat, rough, metallic coated metals," *J. Heat Transf.*, vol. 124, pp. 405–412, 2002.

[5] K. Verma, D. Columbus, B. Han, and B. Chandran, "Real time warpage measurement of electronic components with variable sensitivity," presented at the 1998 ECTC, Seattle, WA.

[6] R. Prasher, "Surface chemistry and characteristic based model for the thermal contact resistance of fluidic interstitial thermal interface materials," *J. Heat Transf.*, vol. 123, pp. 969–975, 2001.

[7] V. C. Zhirnov, R. K. Cavin, III, J. A. Hutchby, and G. I. Bourianoff, "Limits to binary logic switch scaling—A Gedanken model," *Proc. IEEE*, vol. 91, no. 11, pp. 1934–1939, Nov. 2003.

[8] R. Mahajan, C.-P. Chiu, and G. Chrysler, "Cooling a chip: A packaging perspective," *Proc. IEEE*, vol. 94, no. 7, Jul. 2006.

[9] A. Watwe and R. Prasher, "Spreadsheet tool for quick-turn 3-D numerical modeling of package thermal performance with non-uniform die heating," presented at the 2001 ASME Int. Mechanical Engineering Congr. and Exposition, New York, paper 2-16-7-5.

[10] J. Torresola, G. Chrysler, C. Chiu, R. Mahajan, D. Grannes, R. Prasher, and A. Watwe, "Density factor approach to representing die power map on thermal management," *IEEE Trans. Adv. Packag.*, to be published.

[11] R. Mahajan, C.-P. Chiu, and R. Prasher. (2004). Thermal interface materials: A brief review of design characteristics and materials. *Electron. Cooling*. [Online]. *10(1)*. Available: http://www.electronicsooling.com/html/2004_february_a1.html

[12] J. P. Gwinn and R. L. Webb, "Performance and testing of thermal interface materials," in *Proc. Thermes 2002*, Y. K. Joshi and S. V. Garimella, Eds., pp. 307–316.

[13] G. R. Cunnington, Jr., "Thermal conductance of filled aluminum and magnesium joints in a vacuum environment," presented at the ASME Winter Annu. Meeting, New York, 1964, ASME Paper No. 64-WA/HT-40.

[14] R. C. Getty and R. E. Tatro, "Spacecraft thermal joint conduction," presented at the Thermophysics Specialist Conf., New Orleans, LA, 1967, AIAA Paper No. 67-316.

[15] E. E. Marotta and L. S. Fletcher, "Thermal contact conductance of selected polymeric materials," *J. Thermophys. Heat Transf.*, vol. 10, no. 2, pp. 334–342, 1996.

[16] L. S. Fletcher, "A review of thermal enhancement techniques for electronics systems," *IEEE Trans. Compon., Hybrids, Manuf. Technol.*, vol. 13, no. 4, pp. 1012–1021, Dec. 1990.

[17] S. R. Mirmira, E. E. Marotta, and L. S. Fletcher, "Thermal contact conductance of adhesives for microelectronic systems," *J. Thermophys. Heat Transf.*, vol. 11, no. 2, pp. 141–145, 1997.

[18] ——, "Thermal contact conductance of elastomeric gaskets," presented at the 35th

Aerospace Sciences Meeting and Exhibit, Reno, NV, 1997.

[19] E. E. Marotta and B. Han, "Thermal control of interfaces for microelectronic packaging," *Proc. Material Research Soc. Symp.*, 1998, vol. 515, pp. 215–225.

[20] Y. Xu, X. Luo, and D. D. L. Chung, "Sodium silicate based thermal interface material for high thermal contact conductance," *J. Electron. Packag.*, vol. 122, pp. 128–131, 2000.

[21] P. Zhou and K. E. Goodson, "Modeling and measurement of pressure-dependent junction-spreader thermal resistance for integrated circuits," in *Proc. ASME Int. Mechanical Engineering Congr. and Exposition*, 2001, pp. 51–67.

[22] J. J. Fuller and E. E. Morotta, "Thermal contact conducatance of metal/polymer joints: an analytical and experimental investigation," *J. Thermophys. Heat Transf.*, vol. 15, no. 2, pp. 228–238, 2001.

[23] R. S. Prasher, J. C. Shipley, S. Prstic, P. Koning, and J. Wang, "Rheological study of micro particle laden polymeric thermal interface materials: Experimental (part 1) and modeling (part 2)," presented at the Int. Mechanical Engineering Congr. and Exposition, New Orleans, LA, 2002.

[24] R. S. Prasher, P. Koning, J. Shipley, and A. Devpura, "Dependence of thermal conductivity and mechanical rigidity of particle laden polymeric thermal interface materials on particle volume fraction," *J. Electron. Packag.*, vol. 125, no. 3, pp. 386–391, 2003.

[25] R. S. Prasher, J. Shipley, S. Prstic, P. Koning, and J.-L. Wang, "Thermal resistance of particle laden polymeric thermal interface materials," *J. Heat Transf.*, vol. 125, no. 6, pp. 1170–1177, 2003.

[26] R. S. Prasher, "Rheology based modeling and design of particle laden polymeric thermal interface material," presented at the 2004 Intersoc. Conf. Thermal Phenomena, Las Vegas, NV.

[27] R. S. Prasher and J. C. Matayabus, "Thermal contact resistance of cured gel polymeric thermal interface material," *IEEE Trans. Compon. Packag. Technol.*, vol. 27, no. 4, pp. 702–709, Dec. 2004.

[28] E. E. Marotta, S. LaFontant, D. McClafferty, and S. Mazzuca, "The effect of interface pressure on thermal joint conductance for flexible graphite materials: Analytical and experimental study," in *Proc. 2002 Intersoc. Conf. Thermal Phenomena*, 2003, pp. 663–670.

[29] X. Hu, L. Jiang, and K. E. Goodson, "Thermal conductance enhancement of particle-filled thermal interface materials using carbon nanotube inclusions," presented at the 9th Intersoc. Conf. Thermal and Thermomechanical Phenomena in Electronic System, Las Vegas, NV, 2004.

[30] X. Hu, S. Govindasamy, and K. E. Goodson, "Two-medium model for the bond line thickness of particle filled thermal interface materials," presented at the Int. Mechanical Engineering Congr. and Exposition, Anaheim, CA, 2004.

[31] V. Singhal, T. Siegmund, and S. V. Garimella, "Optimization of thermal interface materials for electronics cooling applications," *IEEE Trans. Compon. Packag. Technol.*, vol. 27, no. 2, pp. 244–252, Jun. 2004.

[32] D. P. H. Hassleman and L. F. Johnson, "Effective thermal conductivity of composites with interfacial thermal barrier resistance," *J. Composite Mater.*, vol. 21, pp. 508–515, 1987.

[33] L. C. Davis and B. E. Artz, "Thermal conductivity of metal–matrix composites," *J. Appl. Phys.*, vol. 77, no. 10, pp. 4954–4960, 1995.

[34] C.-W. Nan, R. Birringer, D. R. Clarke, and H. Gleiter, "Effective thermal conductivity of particulate composites with interfacial thermal resistance," *J. Appl. Phys.*, vol. 81, no. 10, pp. 6692–6699, 1997.

[35] J. D. Felske, "Effective thermal conductivity of composite spheres in a continuous medium with contact resistance," *Int. J. Heat Mass Transf.*, vol. 47, pp. 3453–3461, 2004.

[36] H. T. Davis, L. R. Valencourt, and C. E. Johnson, "Transport processes in composite media," *J. Amer. Ceramic Soc.*, vol. 58, no. 9–10, pp. 446–452, 1975.

[37] A. G. Every, Y. Tzou, D. P. H. Hassleman, and R. Raj, "The effect of particle size on the thermal conductivity of ZnS/diamond composites," *Acta Metallurgica et Materialia.*, vol. 40, no. 1, pp. 123–129, 1992.

[38] P. E. Phelan and R. C. Niemann, "Effective thermal conductivity of a thin, randomly oriented composite material," *J. Heat Transf.*, vol. 120, pp. 971–976, 1998.

[39] D. Ganapathy, S. Singh, P. Phelan, and R. S. Prasher, "An effective unit cell approach to compute thermal conductivity of composites with cylindrical particles," *J. Heat Transf.*, 2005, to be published.

[40] A. Devpura, P. E. Phelan, and R. S. Prasher, "Percolation theory applied to the analysis of thermal interface materials in flip-chip technology," presented at the ITHERM, Las Vegas, NV, 1999.

[41] S. Kirkpatrick, "Percolation and conduction," *Rev. Mod. Phys.*, vol. 45, no. 4, pp. 574–588, 1973.

[42] R. Landauer, "Electrical conductivity in inhomogeneous media," *AIP Conf. Proc.*, vol. 40, *Electrical Transport and Optical Properties of Inhomogeneous Media*, J. C. Garland and D. B. Tanner, Eds., no. 1, pp. 2–45, Apr. 1978.

[43] B. Hakansson and R. G. Ross, "Effective thermal conductivity of binary dispersed composites over wide ranges of volume fraction, temperature and pressure," *J. Appl. Phys.*, vol. 68, no. 7, pp. 3285–3292, 1990.

[44] X.-G. Liang, J. R. Lukes, and C.-L. Tien, "Anisotropic thermal conductance in thin layers of disordered packed spheres," in *Proc. 11th Int. Heat Transfer Conf.*, 1998, pp. 33–38.

[45] X.-G. Liang and X. Ji, "Thermal conductance of randomly oriented composites of thin layers," *Int. J. Heat Mass Transf.*, vol. 43, pp. 3633–3640, 2000.

[46] R. Zallen, *The Physics of Amorphous Solids*. New York: Wiley, 1983, pp. 167.

[47] A. E. Morozovskii and A. A. Snarskii, "Finite scaling of the effective conductivity in percolation systems with nonzero ratio of the phase conductivities," *JETP*, vol. 82, no. 2, pp. 361–365, 1996.

[48] J. Wu and D. S. McLachlan, "Percolation exponents and thresholds obtained from the nearly ideal continuum percolation system graphite-boron nitride," *Phys. Rev. B*, vol. 56, no. 3, pp. 1236–1248, 1997.

[49] W. J. Kim, M. Taya, K. Yamada, and N. Kamiya, "Percolation study on electrical resistivity of SiC/Si_3N_4 composites with segregated distribution," *J. Appl. Phys.*, vol. 83, no. 5, pp. 2593–2598, 1998.

[50] A. V. Neimark, "Electrophysical properties of a percolation layer of finite thickness," *Soviet Phys. JETP*, vol. 71, no. 2, pp. 341–349, 1990.

[51] A. Devpura, P. E. Phelan, and R. S. Prasher, "Size effects on the thermal conductivity of polymers laden with highly conductive filler particles," *Microscale Thermophys. Eng.*, vol. 5, no. 3, pp. 177–191, 2001.

[52] P. Keblinski and F. Cleri, "Contact resistance in percolating networks," *Phys. Rev. B*, vol. 69, p. 184201, 2004.

[53] M. Matsukawa, F. Tatezaki, H. Ogasawara, K. Noto, and K. Yoshida, "Thermal transport and percolative transition in the Ag-BPSCCO composite system," *J. Phys. Soc. Jpn.*, vol. 64, no. 1, pp. 164–169, 1995.

[54] K. H. Kim, M. Uehara, C. Hess, P. A. Sharma, and S.-W. Cheong, "Thermal and electronic transport properties and two-phase mixtures in $La_{5/8-x}Pr_xCa_{3/8}MnO_3$," *Phys. Rev. Lett.*, vol. 84, no. 13, pp. 2961–2964, 2000.

[55] H. Hatta and M. Taya, "Effective thermal conductivity of a misoriented short fiber composite," *J. Appl. Phys.*, vol. 58, no. 7, pp. 2478–2486, 1985.

[56] R. C. Progelhof, J. L. Throne, and R. R. Ruetsch, "Methods for predicting the thermal conductivity of composite systems: A review," *Polym. Eng. Sci.*, vol. 16, no. 9, pp. 615–625, 2004.

[57] Y. He, "Rapid thermal conductivity measurement with a hot disk sensor: Part 1. Theoretical considerations," in *Proc. 30th North Amer. Thermal Analysis Soc. Conf.*, 2002, pp. 499–504.

[58] ——, "Rapid thermal conductivity measurement with a hot disk sensor: Part 2. Charecterization of thermal greases," in *Proc. 30th North Amer. Thermal Analysis Soc. Conf.*, 2002, pp. 505–510.

[59] C. L. Kreider, "Silicones," in *Guide to Engineering Plastics*, vol. 2. Metals Park, OH: ASM Int., 1999.

[60] X. Zhang, "Constructive Modeling Strategies and Implementation Frameworks for Hierarchical Synthesis," Ph.D. Thesis, Purdue Univ., West Lafayette, IN, 2004.

[61] R. S. Prasher, O. Alger, and P. E. Phelan, "A unified macroscopic and microscopic approach to contact conduction heat transfer," presented at the 35th Nat. Heat Transfer Conf., Anaheim, CA, 2001.

[62] P. Bujard, G. Kuhnlein, S. Ino, and T. Shiobara, "Thermal conductivity of molding compounds for plastic packaging," *IEEE Trans. Compon., Packag., Manuf. Technol. A*, vol. 17, no. 4, pp. 527–532, Dec. 1994.

[63] P. Bujard, K. Munk, and G. Kuhnlein, "Thermal conductivity of a chain of particles in close contact in a matrix of epoxy resin," *Therm. Conductivity*, vol. 22, pp. 711–722, 1994.

[64] A. V. Shenoy, *Rheology of Filled Polymer System*. Norwell, MA: Kluwer, 1999.

[65] A. Sepehr and M. Sahimi, "Elastic properties of three-dimensional percolation networks with stretching and bond-bending forces," *Phys. Rev. B*, vol. 38, no. 10, pp. 7173–7176, 1988.

[66] T. B. Lewis and L. E. Nielsen, "Dynamic mechanical properties of particulate-filled composites," *J. Appl. Polym. Sci.*, vol. 14, pp. 1449–1471, 1970.

[67] A. K. Das and S. S. Sadhal, "Analytical solution for constriction resistance with interstitial fluid," *Heat Mass Transf.*, vol. 34, pp. 111–119, 1998.

[68] E. Samson, S. Machiroutu, J.-Y. Chang, I. Santos, J. Hermarding, A. Dani, R. Prasher, D. Song, and D. Puffo, "Some thermal technology and thermal management considerations in the design of next

generation Intel Centrino Mobile Technology platforms," *Intel Technol. J.*, vol. 9, no. 1, 2005.

[69] T. L. Tansley and D. S. Maddison, "Conductivity degradation in oxygen polypyrrole," *J. Appl. Phys.*, vol. 69, no. 11, pp. 7711–7713, 1991.

[70] C.-P. Chiu, J. G. Maveety, and Q. A. Tran, "Characterization of solder interfaces using laser flash metrology," *Microelectron. Reliab.*, vol. 42, pp. 93–100, 2002.

[71] L. S. Pritchard, P. P. Acarnley, and C. M. Johnson, "Effective thermal conductivity of porous solder layers," *IEEE Trans. Compon. Packag. Technol.*, vol. 27, no. 2, pp. 259–267, Jun. 2004.

[72] X. Hu, L. Jiang, and K. E. Goodson, "Thermal characterization of eutectic alloy thermal interface materials with void-like inclusions," in *Proc. Annu. IEEE Semiconductor Thermal Measurement and Management Symp.*, 2004, pp. 98–103.

[73] P. Kim, L. Shi, A. Majumdar, and P. L. McEuen, "Thermal transport measurements of individual multiwalled nanotubes," *Phys. Rev. Lett.*, vol. 87, no. 21, pp. 215502-1–215502-4, 2001.

[74] J. Hone, M. C. Llaguno, M. J. Biercuk, A. T. Johnson, B. Batlogg, Z. Benes, and J. E. Fisher, "Thermal properties of carbon nanotubes and nantube-based materials," *Appl. Phys. A, Mater. Sci. Process.*, vol. 74, pp. 339–343, 2002.

[75] M. J. Biercuk, M. C. Llaguno, M. Radosavljevic, J. K. Hyun, A. T. Johnson, and J. E. Fischer, "Carbon nantube composites for thermal management," *Appl. Phys. Lett.*, vol. 80, no. 2, pp. 2767–2769, 2002.

[76] E. T. Thostenson, Z. Ren, and T.-W. Chou, "Advances in the science and technology," *Composite Sci. Technol.*, vol. 61, pp. 1899–1912, 2001.

[77] C. H. Liu, H. Huang, Y. Wu, and S. S. Fan, "Thermal conductivity improvement of silicone elastomer with carbon nanotube loading," *Appl. Phys. Lett.*, vol. 84, no. 21, pp. 4248–4250, 2004.

[78] S. Huxtable, D. G. Cahill, S. Shenogin, L. Xue, R. O. Zisik, P. Barone, M. Usrey, M. S. Strano, G. Siddons, M. Shim, and P. Keblinski, "Interfacial heat flow in carbon nanotube suspensions," *Nature Mater.*, vol. 2, pp. 731–734, 2003.

[79] C.-W. Nan, G. Liu, Y. Lin, and M. Li, "Interface effect on thermal conductivity of carbon nanotube composites," *Appl. Phys. Lett.*, vol. 85, no. 16, pp. 3549–3551, 2004.

[80] J. Xu and T. S. Fisher, "Enhanced thermal contact conductance using carbon nanotube arrays," in *Proc. 2004 Intersoc. Conf. Thermal Phenomena*, pp. 549–555.

[81] ——, "Thermal contact conductance enhancement with carbon nanotube arrays," presented at the 2004 Int. Mechanical Engineering Congr. and Exposition, Anaheim, CA, paper IMECE2004-60185.

[82] X. Hu, A. Padilla, J. Xu, T. S. Fisher, and K. E. Goodson, "Thermal characterization of aligned carbon nanotubes on silicon," presented at the IEEE SEMI-THERM 21, San Jose, CA, 2005.

[83] P. C. Irwin, Y. Cao, A. Bansal, and L. S. Schadler, "Thermal and mechanical properties of polyimide nanocomposites," in *2003 Annu. Report Conf. Electrical Insulation and Dielectric Phenomena*, pp. 120–123.

[84] L. Fan, B. Su, J. Qu, and C. P. Wong, "Effects of nano-sized particles on electrical and thermal conductivities of polymer composites," in *Proc. 9th Int. Symp. Advanced Packaging Materials*, 2004, pp. 193–199.

[85] S. A. Putnam, D. G. Cahill, B. J. Ash, and L. S. Schadler, "High-precision thermal conductivity measurements as a probe of polymer/nanoparticle interfaces," *J. Appl. Phys.*, vol. 94, no. 10, pp. 6785–6788, 2003.

ABOUT THE AUTHOR

Ravi Prasher received the B.Tech. degree in mechanical engineering from the Indian Institute of Technology, Delhi, in 1995 and the Ph.D. degree in mechanical engineering from Arizona State University (ASU), Tempe, in 1999.

After finishing his Ph.D. degree, he joined the Assembly Technology Development division of Intel Corp., Chander, AZ. He is also an Adjunct Professor in the Department of Mechanical and Aerospace Engineering at ASU. He has codeveloped a graduate course on nanoscale energy transport at ASU. He has published approximately 32 archival journal and 35 conference articles and two book chapters in edited volumes. He currently holds 11 patents with 21 patent applications pending with the U.S. Patent Office in the area of microchannels, thin-film thermoelectrics, heat pipes, and thermal interface materials. His primary research and technology development interests are in using nano and micro systems to enhance the conductive, convective and radiative behavior of materials including solids and liquids.

Dr. Prasher is Associate Editor of IEEE TRANSACTIONS ON COMPONENTS AND PACKAGING.